ACS APPLIED MATERIALS & INTERFACES

Research Article

www.acsami.org

Silylated Mesoporous Silica Membranes on Polymeric Hollow Fiber Supports: Synthesis and Permeation Properties

Hyung-Ju Kim,[†] Nicholas A. Brunelli,[†] Andrew J. Brown,[‡] Kwang-Suk Jang,[†] Wun-gwi Kim,[†] Fereshteh Rashidi,[†] Justin R. Johnson,[†] William J. Koros,[†] Christopher W. Jones,*[,†,‡] and Sankar Nair*[,†]

[†]School of Chemical & Biomolecular Engineering, Georgia Institute of Technology, 311 Ferst Drive, Atlanta, Georgia 30332-0100, United States

[‡]School of Chemistry and Biochemistry, Georgia Institute of Technology, 901 Atlantic Drive, Atlanta, Georgia 30332-0400, United States

Supporting Information

ABSTRACT: We report the synthesis and organic/water separation properties of mesoporous silica membranes, supported on low-cost and scalable polymeric (polyamide-imide) hollow fibers, and modified by trimethylsilylation with hexamethyldisilazane. Thin (~1 μm) defect-free membranes are prepared, with high room-temperature gas permeances (e.g., 20 000 GPU for N_2). The membrane morphology is characterized by multiple techniques, including SEM, TEM, XRD, and FT-ATR spectroscopy. Silylation leads to capping of the surface silanol groups in the mesopores with trimethylsilyl groups, and does not affect the integrity of the mesoporous silica structure and the underlying hollow fiber. The silylated membranes are evaluated for pervaporative separation of ethanol (EtOH), methylethyl ketone (MEK), ethyl acetate (EA), *iso*-butanol (*i*-BuOH), and *n*-butanol (*n*-BuOH) from their dilute (5 wt %) aqueous solutions. The membranes show separation factors in the range of 4−90 and high organic fluxes in the range of 0.18−2.15 kg m^{-2} h^{-1} at 303 K. The intrinsic selectivities (organic/water permeability ratios) of the silylated membranes at 303 K are 0.33 (EtOH/water), 0.5 (MEK/water), 0.25 (EA/water), 1.25 (*i*-BuOH/water), and 1.67 (*n*-BuOH/water) respectively, in comparison to 0.05, 0.015, 0.005, 0.08, and 0.14 for the unmodified membranes. The silylated membranes allow upgradation of water/organics feeds to permeate streams with considerably higher organics content. The selective and high-flux separation is attributed to both the organophilic nature of the modified mesopores and the large effective pore size. Comparison with other organics/water separation membranes reveals that the present membranes show promise due to high flux, use of scalable and low-cost supports, and good separation factors that can be further enhanced by tailoring the mesopore silylation chemistry.

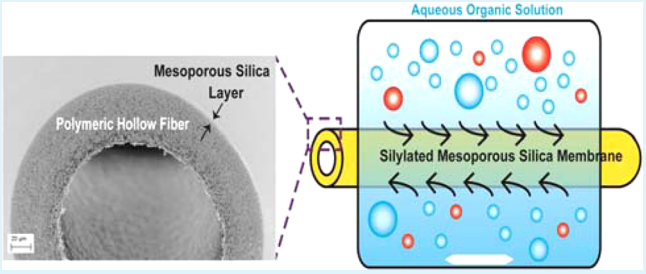

KEYWORDS: *mesoporous silica, membrane, hollow fiber, silylation, organics/water separation*

1. INTRODUCTION

Membrane-based separations are becoming increasingly competitive for a number of applications, such as hydrogen recovery, air separation, CO_2 separation, and organics recovery[1−3] due to their low energy requirements, potentially low fabrication cost, and steady-state operation. Polymeric membranes (e.g., in the form of hollow fibers) are amenable to large-scale fabrication processes and typically have large surface area to volume ratios (>1000 m^2/m^3).[4] However, they also have an intrinsic "upper bound" on their performance, reflecting a trade-off between their permeability and selectivity.[5,6] Although the trade-off is well-studied in the context of gas separations, it also exists in organics/water separations.[7−10] Such separations are of importance in the production of biofuels, biobased chemicals, pharmaceuticals, and biomolecules.[11−13] In many cases, it is desired to recover the organic molecules from an aqueous dilute solution. The availability of an efficient and low-cost membrane platform capable of upgrading these dilute solutions to higher concentrations would improve the economics of the above processes. The upgraded streams could then be further purified by more conventional processes to remove the remaining water (e.g., drying/adsorption with hydrophilic molecular sieves or membrane separations with hydrophilic polymer membranes).[14,15]

Over the past decade, inorganic membranes have been shown to possess high permeability, tunable selectivity, and good thermal and chemical resistances.[16−20] Their widespread application is yet limited by the difficulty of fabricating them in a technologically scalable and low-cost manner. Certain types of hydrophilic zeolite membranes have successfully been fabricated on polymeric support tubes, and show excellent

Received: July 13, 2014
Accepted: September 25, 2014
Published: September 25, 2014

separation factors for water over organics of over 10 000.[17] These membranes address the "finishing step" of dehydration from an already concentrated product, but not the initial upgrading step from a dilute feed stream. For the latter case, several researchers have investigated the use of nanocomposite membranes that combine a hydrophobic and permeable polymer (typically a silicone elastomer) with hydrophobic molecular sieves such as pure-silica MFI.[21−23] Such membranes can potentially be scaled up to spiral-wound modules.[24] However, to our knowledge there is currently no reliable method of producing these membranes on high-surface-area platforms such as hollow fibers.

In this work, we have taken a different approach toward a more scalable membrane platform for organic/water separations. Recently, we demonstrated that continuous mesoporous silica membranes can be fabricated on polymeric hollow-fiber supports using facile and low-temperature chemistry.[25] Mesoporous silica materials prepared using long-chain surfactant templates have worm-like pore channels with a diameter range of 2−10 nm. The mesopores allow for rapid diffusion of target molecules, and can be modified[26−31] in a variety of ways to impart selectivity to the permeation characteristics, thereby allowing for specific separation applications over a range of molecular sizes. Mesoporous silica membranes have been proposed as potential candidates for separation applications. Such membranes have been synthesized on ceramic substrates[32−36] and modified further to tailor the selective properties.[32−40] For example, Kumar synthesized an MCM-48 membrane on α-alumina, functionalized it with poly(ethylenimine), and used it for CO_2/N_2 separations.[41] Nishiyama modified an MCM-48 membrane with trimethylchlorosilane groups and studied the separation of organic/water mixtures.[42] Recently, we reported a seeded growth technique for MCM-48 membranes on α-alumina, and their subsequent silylation for use in organic/water separations.[43] Here we report the fabrication, characterization, and permeation properties of thin (∼1 μm) silylated mesoporous silica membranes on poly(amide-imide) hollow fibers. We characterize in detail the structure and composition of the mesoporous silica membrane. Pervaporation of five different organic/water mixtures is studied to understand the permeation characteristics of the silylated mesoporous membranes. The effects of temperature on the separation performance, and the mechanism of separation with the silylated mesoporous silica hollow fiber membranes, are also discussed.

2. EXPERIMENTAL SECTION

2.1. Mesoporous Membrane Synthesis and Characterization. *2.1.1. Materials.* The following chemicals were used as received: tetraethylorthosilicate (TEOS, 98% Sigma-Aldrich), cetyltrimethylammonium bromide (CTAB, Sigma-Aldrich), 1 N aqueous hydrochloric acid (HCl) solution (Sigma-Aldrich), hexamethyldisilazane (HMDS, Alfa Aesar), ethanol (EtOH, BDH), methylethyl ketone (MEK, Sigma-Aldrich), ethyl acetate (EA, Sigma-Aldrich), *iso*-butanol (*i*-BuOH, EMD), *n*-butanol (*n*-BuOH, Sigma-Aldrich), and Torlon 4000T-LV (Solvay Advanced Polymers).

2.1.2. Mesoporous Silica Membrane Coating on Torlon Hollow Fibers. Macroporous Torlon poly(amide-imide) hollow fiber supports were fabricated by a dry-jet/wet-quench method, described in detail by us elsewhere.[44] The outer and inner diameters of the support fibers were ca. 380 and 230 μm, respectively. The fibers did not possess skin layers and had open pores of ∼100 nm size at the outer surface. The mesoporous silica membrane was fabricated as described in our previous report.[25] Before the membrane coating, both ends of the fiber support were sealed with epoxy to prevent the membrane growth in the interior of the fiber support. The support Torlon hollow fibers were immersed in the coating solution for 5 h at room temperature. The mixture had the molar composition of 1 TEOS: 0.425 CTAB: 0.00560 HCI: 62.2 H_2O. The prepared hollow fiber membranes were aged with saturated TEOS vapor prior to use. A 22 cm-long fiber membrane was placed with 25 μL of TEOS in a closed vessel at 373 K for 24 h. For surfactant extraction, the fiber membranes were washed with 0.05 N HCl/ethanol under stirring for 24 h at 298 K.

2.1.3. Silylation of Mesoporous Membrane. Prior to silylation, the surfactant-extracted mesoporous silica membranes were evacuated in a vacuum oven at 423 K under 0.07 atm, to remove physically adsorbed moisture and residual surfactant. Then, the membranes were exposed to HMDS vapor in a closed vessel at 373 K for 24 h. After silylation, the membranes were washed with deionized water at 298 K for 30 min in a separate container under stirring. Then, the coated membranes were dried at 363 K before preparing the pervaporation measurement module.

2.1.4. Characterization Methods. Scanning electron microscopy (SEM) was performed with a LEO 1530 instrument to examine the membranes. The membrane samples were prepared on carbon tape and coated with gold to prevent surface charging. X-ray diffraction (XRD) patterns of the membranes were obtained by a PANalytical X'pert diffractometer using a Cu−K-alpha X-ray source, diffracted beam collimator, and a proportional detector. For XRD, the samples were aligned on the center of an aluminum mount and attached to the surface with double-sided tape. FT-ATR (Attenuated total reflectance)/IR spectra were obtained using a Bruker Vertex 80v Fourier Transform Infrared (FT-IR) spectrometer coupled to a Hyperion 2000 IR microscope at 20× magnification. High-resolution transmission electron microscopy (TEM) was performed on a FEI Tecnai G^2 F30 TEM at 300 kV. TEM samples were prepared after dissolving away the support fiber using *N*,*N*-dimethylformamide. On the basis of the TEM images, pore sizes were estimated using the NIH ImageJ software. In the selected area of worm-like mesopores, the pore size can be estimated by recognizing the pores as particles and using their width and height given by ImageJ.[45,46]

2.2. Gas Permeation and Pervaporation Measurements. Gas permeation was measured using a hollow fiber permeation testing system, constructed in-house as described earlier.[47,48] Gases were fed into the bore ("tube side") of the fiber interior at one end of the module (single fiber of 15.5 cm length). The temperature of the system was maintained at 308 K during the measurement. The flux through the fiber walls was measured on the "shell side" connected to a bubble flow meter. Atmospheric pressure was maintained on the downstream side. The flux was converted to permeance and permeability.[49] Permeances are expressed in GPUs (Gas Permeation Units, 1 GPU = 10^{-6} cm^3 (STP) cm^{-2} s^{-1} $cmHg^{-1}$) and permeabilities are given as Barrers (1 Barrer = 10^{-10} cm^3 (STP) cm cm^{-2} s^{-1} $cmHg^{-1}$). Pervaporation measurements were carried out using an aqueous mixture of a specific organics (5 wt % organic) at 303 and 323 K using a custom-built unit. The single-fiber membrane was assembled into a pervaporation module of 18 cm length. The permeate vapor was condensed in a liquid nitrogen-cooled trap under vacuum conditions, over a period of up to 10 h. The total flux was obtained from the mass of permeate collected in a given measurement time, and its composition was characterized by gas chromatography (GC) and ^1H NMR (nuclear magnetic resonance) in deuterated acetone. The gas permeance of any component i is expressed as its flux normalized by its transmembrane partial pressure:

$$P_i = \frac{N_i}{\Delta p_i} \tag{1}$$

The theoretical Knudsen permeance is calculated by the following equation:

$$P_i = \frac{1}{RT}\frac{g}{\delta}D_{Kn} \tag{2}$$

Here R is the gas constant, T is temperature, g is the porosity (ε)-to-tortuosity (τ) ratio of the support, δ is the membrane thickness, and

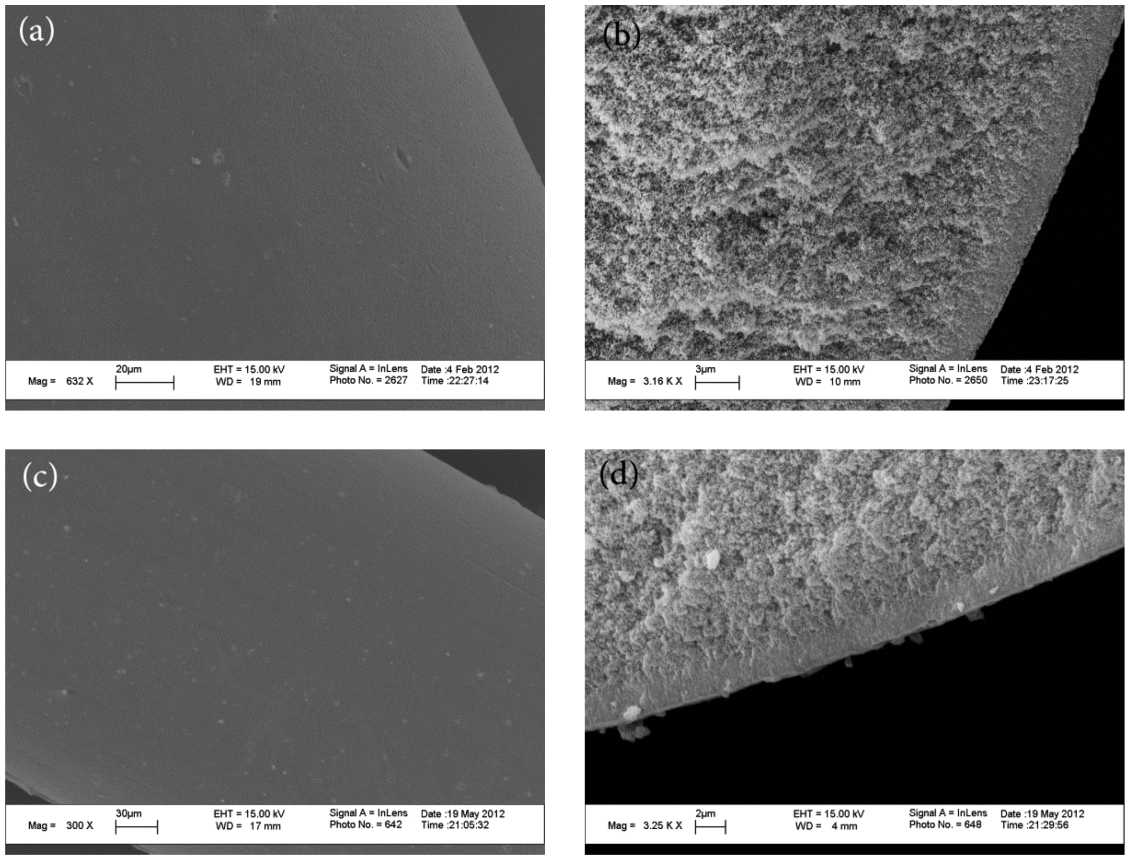

Figure 1. SEM images of (a) top view and (b) cross section of evacuated mesoporous silica/Torlon hollow fiber membranes; and (c) top view and (d) cross section of HMDS-silylated mesoporous silica/Torlon hollow fiber membranes.

D_{Kn} is the Knudsen diffusivity. Permeability is calculated by multiplying the permeance by the membrane thickness. The ideal selectivity of the membrane is the ratio of the permeances of each species. For binary mixtures of components A and B, the ideal selectivity is described by the following:

$$\alpha_{A/B} = \frac{P_A}{P_B} \tag{3}$$

The separation factor is the ratio of molar component concentrations in the fluids on either side of the membrane:

$$\beta_{A/B} = \frac{c_{A_p}/c_{B_p}}{c_{A_f}/c_{B_f}} \tag{4}$$

where c_{A_p} is the molar concentration of A on the permeate side, and c_{A_f} is molar ratio of A on the feed side.

3. RESULTS AND DISCUSSION

3.1. Synthesis, Evacuation, and Silylation of Mesoporous Membrane. Figure 1a,b shows the SEM images of the mesoporous silica/Torlon hollow fiber membranes after evacuation. Continuous silica layers were obtained in a reproducible manner. The precise determination of the membrane thickness is complicated by the fact that the mesoporous silica membrane is present both on top of, as well as interpenetrated with, the underlying Torlon support. In our previous work, the "total" membrane thickness was determined to be about 1.6 μm by slowly dissolving away the Torlon support in a suitable solvent and examining the remaining thin mesoporous silica "skin" by SEM.[25] This method is tedious and difficult to apply at multiple locations of the fiber. Alternatively, we determine here an "apparent" membrane thickness by direct SEM observation of the as-made fiber membrane cross sections at multiple locations along a 3 cm length of the fiber. The apparent thickness is measured from the SEM image by visual observation of the dense silica skin. The thickness at each axial location was obtained by averaging measurements from at least three points on the fiber circumference. Supporting Information (SI) Figure S1 shows the membrane thickness determined in this manner, giving an average thickness of 0.9 ± 0.2 μm. Figure 1c,d shows the SEM images of the HMDS-silylated mesoporous silica/Torlon hollow fiber membranes. The silica layers are not damaged by silylation, and there is no substantial change in the membrane thickness or morphology after silylation. Furthermore, the Torlon hollow fiber supports remained stable without any significant change in their cylindrical morphology during the membrane fabrication and silylation process (SI Figure S2).

Figure 2 shows single gas permeation data at 308 K for the extracted, evacuated, and subsequently silylated mesoporous silica/Torlon hollow fiber membranes at varying feed pressures. Compared to the nonevacuated membrane reported earlier,[25] the permeances of the evacuated membranes increase from 3300 to 20 000 GPU for N_2 and from 4400 to 18 000 GPU for CO_2. This indicates successful removal of adsorbed water and other species at 423 K. Moreover, the relative permeance of N_2 and CO_2 (1.11) is closer to the Knudsen ratio. (Knudsen ratio: N_2/CO_2 = 1.25). Removal of residual species by evacuation activates the mesopores properly for subsequent pore modification. Permeances of N_2 and CO_2 decrease substantially after silylation, consistent with reduction in pore size,

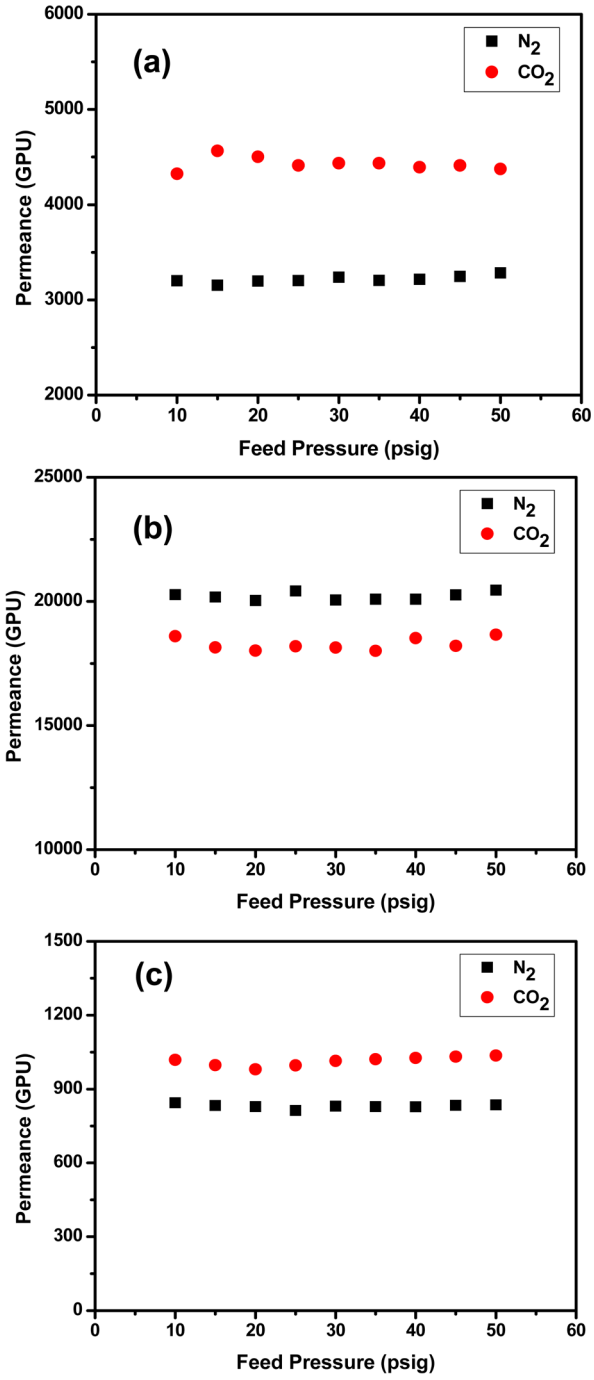

Figure 2. N_2 and CO_2 single-gas permeances at 308 K as a function of feed pressure for (a) template extracted, (b) evacuated, and (c) silylated mesoporous silica/Torlon hollow fiber membranes.

diffusivity, or adsorption strength due to pore functionalization with trimethylsilyl groups. As in the case of the template-extracted and evacuated membranes, the silylated mesoporous membranes have a constant permeance regardless of feed pressure, consistent with gas molecule transport being governed by a Knudsen-like mechanism.[25,43]

Surprisingly, a significant reduction of gas permeance may also be attributed to silylation of the support. As shown in SI Figure S3, the silica-free support also has a reduced permeance (~10 000 GPU) after silylation. According to energy-dispersive X-ray spectroscopy analysis (Figure 3(a)), silicon species are detected on the outer surface of the Torlon hollow fiber, which otherwise should not contain any silicon. Presumably, the amide group in the Torlon structure is also silylated by HMDS,[50] as shown in the scheme of Figure 3(b). The theoretical permeances under conditions for Knudsen-like transport are estimated (N_2 = 47 000 GPU, CO_2 = 38 000 GPU), using the structural tortuosity factor of 3 for the mesoporous silica membrane.[43] The theoretical estimate can be further corrected for the presence of significant gas−solid interactions (i.e., adsorption of gases on the mesopore walls) rather than an ideal Knudsen mechanism.[43] This correction is based on parameters from Bhatia et al.[51,52] for silica mesopores of approximately 3 nm diameters. The corrected theoretical permeances are 23 500 GPU for N_2 and 19 000 GPU for CO_2, which are slightly higher than those for the evacuated membrane. The slight deviation is probably due to pore constrictions or dense material at the mesoporous silica/Torlon interface. On the basis of both the gas permeation measurements and comparison to theoretical values, it is clear that mesoporous silica membranes on hollow fiber supports are successfully fabricated in a controlled manner.

The pore structure of the mesoporous silica membrane was investigated in further detail by XRD and TEM imaging. Figure 4 shows the low-angle XRD patterns of the mesoporous silica membranes at several stages of processing (template-extracted, evacuated, and silylated). Although an intense diffraction signal is difficult to obtain due to the curved surface of the sample and the thin membrane layer, the existence of mesoporous silica is clearly indicated. The increase (Figure 4b) and decrease (Figure 4c) in peak intensity due to evacuation and silylation of the template-extracted membrane (Figure 4a) are due to the changes of electron density contrast between the mesopores and the silica walls, consistent with removal of residual species and modification of the pores with trimethylsilyl species, respectively.

The silica layers of the same set of membranes were examined by TEM (Figure 5) after dissolving away the Torlon support fiber. The remaining silica structure containing worm-like channels was observed for the membranes in each stage. Moreover, image analysis results for the height and width of the pores show that the pore size is consistent with the presence of a mesoporous material with a diameter of about 2 nm (SI Figures S4, S5, and S6). The pores of template-extracted (SI Figure S4) and silylated (SI Figure S6) membranes appear to be slightly smaller than those of the evacuated (SI Figure S5) mesoporous membrane, qualitatively indicating the reduction of the size of the pore channels due to the presence of surfactants and trimethylsilyl species. This analysis is consistent with the gas permeation measurements.

FT-ATR/IR was used to investigate the modification of the silica layer. Figure 6 shows the ATR/IR spectra of a mesoporous silica membrane at different stages of processing. The prepared samples were mounted on the poly(styrene) (PS) plates. One of the PS plates is measured to ensure that the ATR crystal was in proper contact with the samples. The absorption peak around 1080 cm^{-1} is associated with the symmetric and asymmetric stretching vibrations of Si—O—Si linkages in mesoporous silica. After silylation of the mesoporous membrane, the intensity of this peak is significantly increased, which is likely due to the creation of additional Si—O—Si linkages by silylation. Also, the absorption peak around 800 cm^{-1} is more intense as compared to the template-extracted membrane. However, a relatively broad absorption peak located at 3200−3600 cm^{-1} is found in

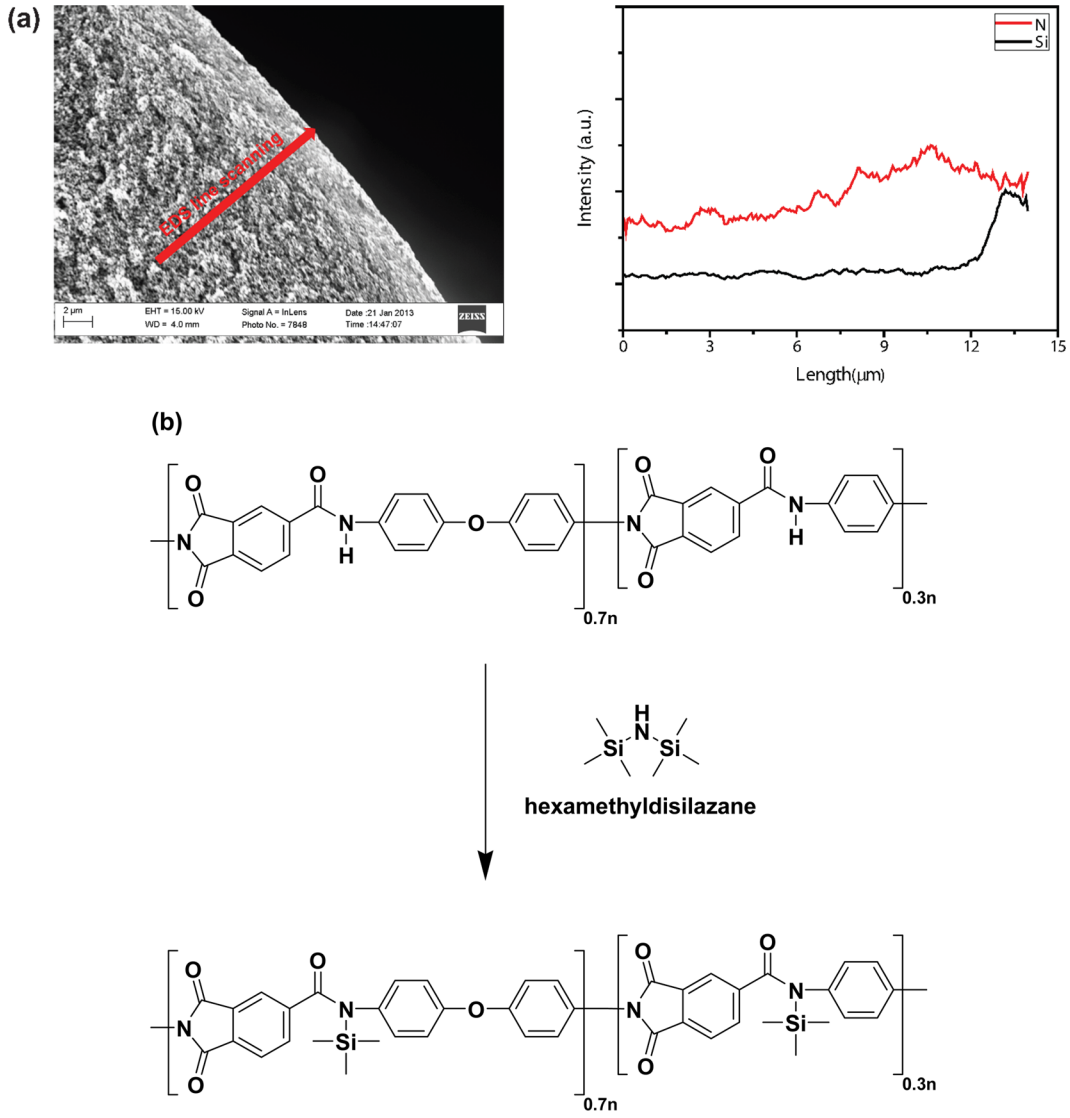

Figure 3. (a) Line scanning analysis of energy-dispersive X-ray spectroscopy (EDS) for the silylated Torlon hollow fiber, and (b) anticipated silylated Torlon structure.

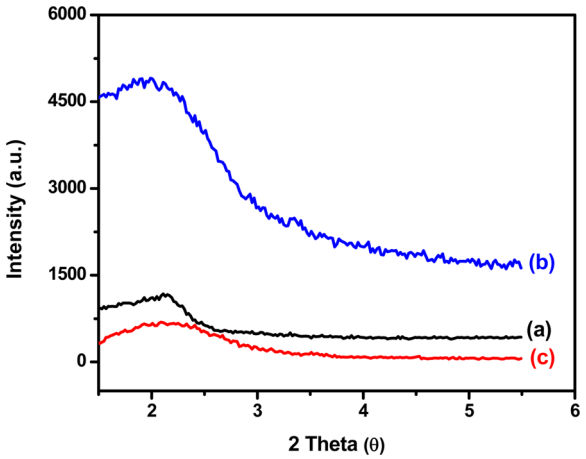

Figure 4. XRD patterns of (a) template-extracted, (b) evacuated, and (c) silylated mesoporous membranes.

the template-extracted and evacuated membranes due to O—H stretching vibrations of the silanol groups and water molecules on the pore walls. These peaks completely disappear after silylation, suggesting that the surface silanols have been eliminated by condensation with the trimethylsilyl groups.[53]

3.2. Pervaporation. Pervaporation data for five different organic/water mixtures are summarized in Figure 7 and SI Figures S7 and S8. To allow a comprehensive understanding of the permeation properties,[54] the data are expressed in terms of flux, organic/water separation factor, permeance, permeability, and water/organic selectivity for template-extracted membranes, evacuated membranes, and silylated membranes, respectively. The permeability in SI Figures S7 and S8 is calculated by multiplying the permeance with the "total" membrane thickness of 1.6 μm[25] (discussed in Section 3.1), and can be easily converted to any other basis, e.g., the apparent thickness of 0.9 μm obtained from SI Figure S1. The feed mixtures used were (5/95 w/w) EtOH/water, MEK/water, EA/water, *i*-BuOH/water, and *n*-BuOH/water. Pervaporation was performed at 303 and 323 K.

Figures 7a,b show the fluxes and *organics-over-water* separation factors from the mixture pervaporation experiments. Beyond the model solutions composed of MEK/water or EA/

dx.doi.org/10.1021/am504581j | ACS Appl. Mater. Interfaces 2014, 6, 17877−17886

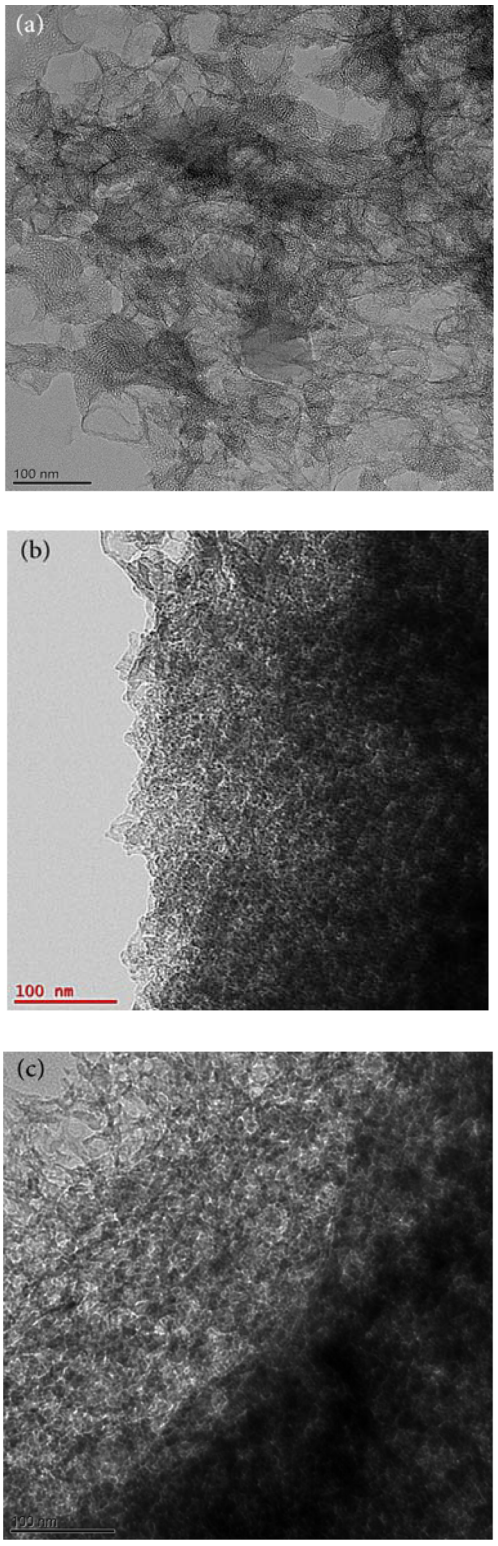

Figure 5. TEM images of the (a) template-extracted, (b) evacuated, and (c) silylated mesoporous membrane layers after dissolution of the Torlon fiber.

water, the hydrophobic mesoporous membranes are also investigated for BuOH/water separations, due to the emerging importance of BuOH as a liquid fuel.[55] Both organic and water fluxes increase with temperature, but it is noteworthy that the water flux increases more than the organic flux. The separation factors of all the organic/water mixtures through the evacuated

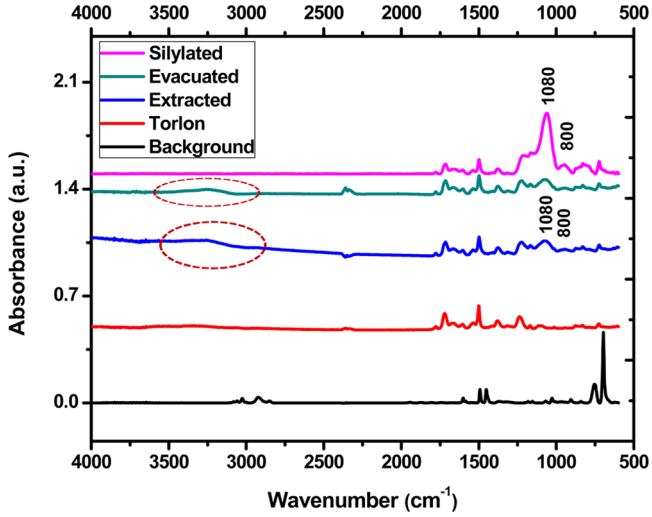

Figure 6. FT-ATR/IR absorption spectra of mesoporous silica/Torlon hollow fiber membranes. The background spectrum is from the PS plate.

membranes range from 0.5 to 1.5, indicating that the membranes are not selective. They permeate almost the same amount of water and organic as is present in the feed mixture. However, the separation factor increases substantially after silylation, as this treatment renders the pore surface hydrophobic via modification by trimethylsilyl groups. The total fluxes somewhat increase or are maintained constant after silylation, and this is caused by a large increase in the fluxes of the organic species after silylation. The separation factors (*organics-over-water*) of the HMDS-treated mesoporous membrane at 303 K vary with the organic components in the order: EA (90) > MEK (19) > *i*-BuOH (13) > *n*-BuOH (11) > EtOH (4). However, higher water fluxes lead to decreased separation factors at the higher temperature of 323 K.

Figure 7c,d shows the permeances and *water-over-organic* selectivities (ratio of water and organic component permeances) for the two membranes, calculated from the membrane transport equation for any component i:

$$J_i = (P_{m,i})(\gamma_i x_i p_i^{sat} - y_i p_p) \quad (5)$$

where J_i is the molar flux of component i, $P_{m,i}$ the permeance, γ_i the activity coefficient, x_i the feed mole fraction, p_i^{sat} the saturated vapor pressure, y_i the permeate mole fraction, and p_P the permeate pressure. Interestingly, the permeances of the organic species do not change much with increasing temperature, whereas the permeance of water increases significantly at 323 K. This result indicates that the permeance of the organic species is more highly dependent on adsorption into the mesopores rather than diffusivity in the mesopores. Even though the silylated mesoporous membrane has high organic fluxes and high organic separation factors (Figure 7b), it still has intrinsic water/organic selectivity in the range of 0.5−4 at 303 K. This is because the original nonsilylated mesoporous membrane is highly hydrophilic and water selective. In other words, the trimethylsilyl groups are able to drastically decrease the flux of water through the membrane, but it still remains on the same order of magnitude as the organic fluxes. For completeness, SI Figure S7 shows the same information as Figure 7c,d, except that the permeability is displayed instead of permeance. It is seen that the silylated membranes display high permeabilities (ranging from 1000 to 15 000 Barrer) for the

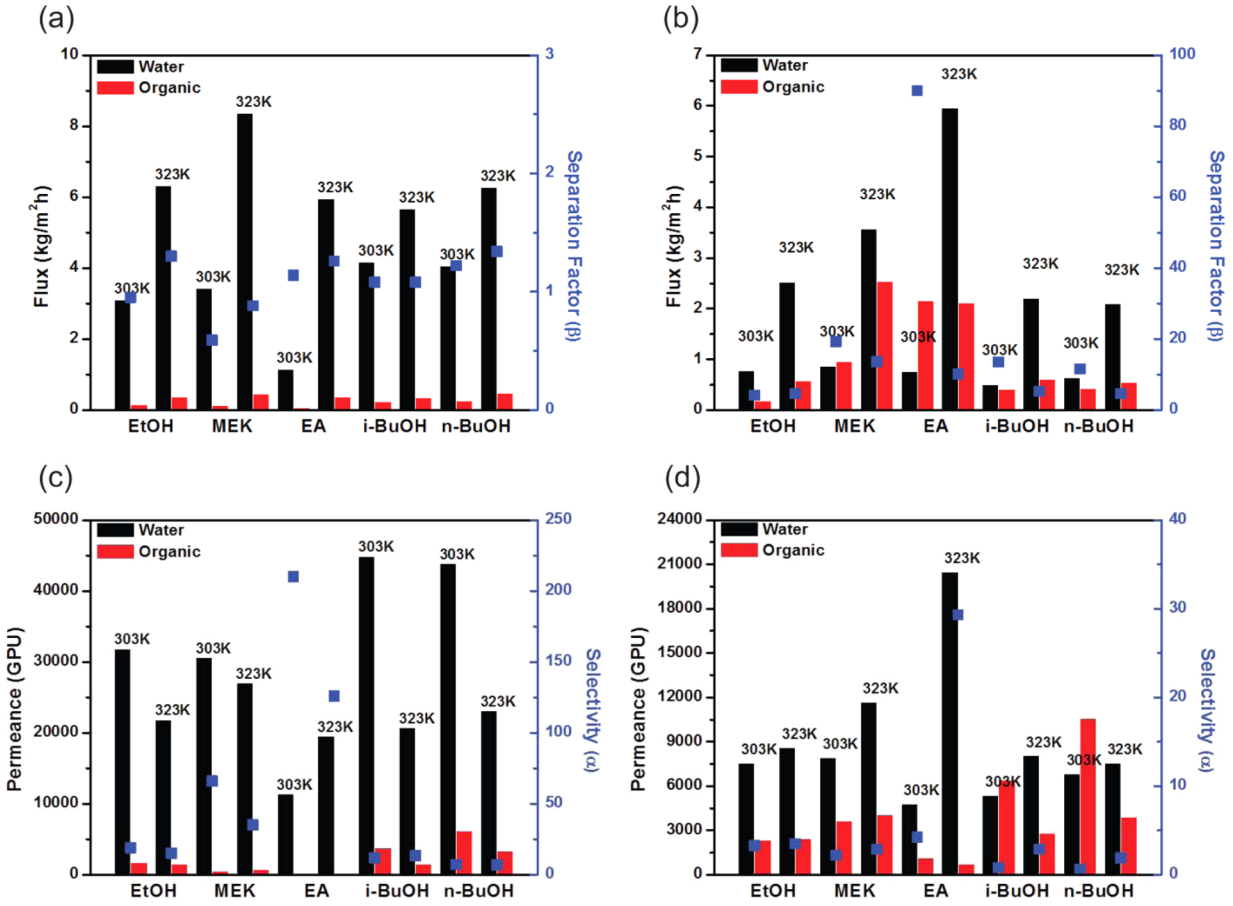

Figure 7. Pervaporation data (flux and organics/water separation factor) at 303 and 323 K with 5 wt % organic/water feeds for (a) evacuated mesoporous membrane, and (b) silylated mesoporous membrane. Pervaporation data (permeance and water/organic selectivity) with 5 wt % organics/water feed mixtures for (c) evacuated mesoporous membrane, and (d) silylated mesoporous membrane.

organic species. SI Figure S8 shows pervaporation data for the template-extracted mesoporous membrane. Similar to the evacuated membrane, the extracted membrane shows low organic separation factors (1−2.5) and high water selectivities (6−130). However, it has a significantly lower flux and permeance, because the residual surfactants and solvents partially block permeation.

As a result of the pervaporation properties discussed above, we find that the present silylated mesoporous silica/Torlon hollow fiber membranes are able to upgrade 5 wt % organic/water feed mixtures to 19% EtOH, 53% MEK, 83% EA, 45% *i*-BuOH, and 40% *n*-BuOH permeate streams in a single pass at 303 K (Table 1). As shown in Table 1, this separation performance is considerably better than that of the evacuated membranes, and also (for completeness) the template-extracted mesoporous silica membranes (SI Table S1).

Table 1. Concentration Upgrades from Feed to Permeate at 303 K

	evacuated membrane		silylated membrane	
feed solution	feed (wt %)	permeate (wt %)	feed (wt %)	permeate (wt %)
EtOH/water	4.7	4.7	5.4	19.1
MEK/water	6.0	3.6	5.4	52.6
EA/water	4.4	5.0	5.1	82.8
i-BuOH/water	5.2	5.6	5.7	44.7
n-BuOH/water	4.8	5.8	5.4	39.8

In Table 2, the present membranes are compared to other classes of hydrophobic membranes recently applied for organic/water pervaporation as reported in the literature. The membranes listed in Table 2 were operated at temperatures in the range of 283−353 K, with feed concentrations in the range of 0.2−30 wt % organics. The comparison focuses on two quantities of interest: the total flux through the membrane (F, in kg·m^{-2}h^{-1}) and the organic/water separation factor (β). Polymeric membranes show the trade-off between flux and separation factor. The fluxes are very low for the membranes that have high separation factors, and vice versa.[56−60] Hydrophobic zeolite membranes supported on ceramic hollow fibers,[61] or on tubular and disk supports,[62−65] can show high performance in both flux and separation factors. Two issues in the application of zeolite membranes are the high cost of ceramic hollow fiber or tubular supports, and the uncertain reliability of hydrothermal synthesis and high-temperature calcination steps for large-scale fabrication. Composite membranes can combine the properties of polymers and zeolites, yielding improved performance over polymers.[23,66,67] However, the scale-up of such membranes to high-surface-area modules is an ongoing research topic. Mesoporous silica membranes prepared on ceramic supports[42,43,53] by hydrothermal synthesis also face the same cost and fabrication challenges as zeolite membranes. The present silylated mesoporous silica membranes are directly prepared on porous

Table 2. Comparison of Organophilic Membranes in Organics/Water Pervaporation[a]

material type	membrane	molecule	F (kg·m^{-2}h^{-1})	β	ref #
polymers	commercial PDMS (Sulzer)	EtOH	0.8	2	56
	PDMS	MEK	0.06	100	57
	PDMS/PVDF	EtOH	0.45	15	58
	chitosan/PVP	EtOH	0.5	250	59
	PVDF-HFP	EA	1.9	180	60
ceramic-supported zeolites	MFI on YSZ hollow fiber	EtOH	7.4	47	61
	B-ZSM-11	MEK	0.6	220	62
	silicalite	EtOH	0.04	35	63
	silicalite	*n*-BuOH	0.04	440	64
	silicalite	MEK	0.25	32000	65
polymer-zeolite nanocomposites	PDMS/silicalite	*n*-BuOH	9.5	104	66
		EtOH	0.06	10	
		n-BuOH	0.04	70	
	PDMS/silicalite	*i*-BuOH	5−11	25−42	67
mesoporous silica	silylated MCM-48 on alumina	EA	4.3	251	53
	silylated MCM-48 on alumina	EtOH	0.26	11	42
		MEK	1.4	201	
		EA	6.2	351	
	silylated MCM-48 on alumina	EtOH	0.15	3	43
		MEK	0.52	10	
		EA	0.55	17	
	silylated mesoporous silica on Torlon hollow fiber	EtOH	1	4	this work
		MEK	1.8	19	
		EA	2.9	90	
		i-BuOH	0.9	13	
		n-BuOH	1.06	11	

[a]PDMS: Polydimethylsiloxane, PVDF: polyvinylidene fluoride, PVP: polyvinylpyrrolidone, HFP: hexafluoropropene.

polymeric hollow fiber supports and can potentially be scaled up to large surface areas. As seen from Table 2, silylation with HMDS already produces mesoporous silica hollow fiber membranes with high organic fluxes and good separation factors. The availability of a number of different mesoporous oxide materials, organic functionalization agents, and techniques for organic functionalization of mesoporous materials, creates optimism that membranes with higher performance can be attained. Significant work remains to be done in understanding the stability of the membranes under long-term operation (beyond the maximum of 10 h reported in this work), and in optimizing mesoporous oxide materials and silylation techniques suited for specific applications. However, the availability of a benign (e.g., not requiring hydrothermal synthesis or calcination) membrane fabrication and functionalization process on a low-cost and scalable support material, as shown in this work, is expected to be advantageous.

4. CONCLUSIONS

Silylated mesoporous silica membranes coated on polymeric hollow fiber supports have been demonstrated for the first time, thereby suggesting a scalable membrane platform for organics recovery. The bare mesoporous silica membranes have high gas permeance (e.g., ∼20 000 GPU for N_2). Hydrophobic trimethylsilyl groups are successfully incorporated on the surfaces of the mesopores, and the mesoporous silica layer remains intact and defect-free, based on XRD, electron microscopy (SEM and TEM), FT-ATR/IR, and gas permeation measurements. The silylated mesoporous membranes are selective for permeation of organic molecules in aqueous EtOH/water, MEK/water, EA/water, *i*-BuOH/water, and *n*-BuOH/water pervaporation experiments, whereas the bare membranes are selective for water. The good separation performance in organic/water mixtures can be attributed primarily to the hydrophobic nature of the silylated pores and the preferential adsorption of organics in the membrane. In relation to other types of organics/water separation membranes, the performance of the present membranes is quite promising for a range of potential organic/water separations. An important advantage of the present mesoporous silica/Torlon hollow fiber membranes is their scalable and low-cost processing methodology. Due to the available range of mesoporous materials, functionalizing agents, and mesopore modification techniques for specific applications, it is quite possible that the membrane performance and long-term stability can be greatly enhanced.

■ ASSOCIATED CONTENT

Supporting Information

Membrane thickness data, low-magnification SEM images of the membranes, pore size distribution analysis methods, single gas permeation data, pore size distribution data, and pervaporation data. This material is available free of charge via the Internet at http://pubs.acs.org/.

■ AUTHOR INFORMATION

Corresponding Authors

*E-mail: sankar.nair@chbe.gatech.edu.
*E-mail: christopher.jones@chbe.gatech.edu.

Notes

The authors declare no competing financial interest.

■ ACKNOWLEDGMENTS

This work was supported by Phillips 66 Company.

REFERENCES

(1) Bernardo, P.; Drioli, E.; Golemme, G. Membrane Gas Separation: A Review/State of the Art. *Ind. Eng. Chem. Res.* **2009**, *48*, 4638−4663.
(2) Striemer, C. C.; Gaborski, T. R.; McGrath, J. L.; Fauchet, P. M. Charge- and Size-Based Separation of Macromolecules Using Ultrathin Silicon Membranes. *Nature* **2007**, *445*, 749−753.
(3) Vankelecom, I. F. J. Polymeric Membranes in Catalytic Reactors. *Chem. Rev.* **2002**, *102*, 3779−3810.
(4) Strathmann, H. Membrane Separation Processes: Current Relevance and Future Opportunities. *AIChE J.* **2001**, *47*, 1077−1087.
(5) Robeson, L. M. Correlation of Separation Factor Versus Permeability for Polymeric Membranes. *J. Membr. Sci.* **1991**, *62*, 165−185.
(6) Robeson, L. M. The Upper Bound Revisited. *J. Membr. Sci.* **2008**, *320*, 390−400.
(7) Gonzalez-Marcos, J. A.; Lopez-Dehesa, C.; Gonzalez-Velasco, J. R. Effect of Operation Conditions in the Pervaporation of Ethanol−Water Mixtures with Poly(1-Trimethylsilyl-1-Propyne) Membranes. *J. Appl. Polym. Sci.* **2004**, *94*, 1395−1403.
(8) Jian, K.; Pintauro, P. N.; Ponangi, R. Separation of Dilute Organic/Water Mixtures with Asymmetric Poly(Vinylidene Fluoride) Membranes. *J. Membr. Sci.* **1996**, *117*, 117−133.
(9) Karlsson, H. O. E.; Tragardh, G. Pervaporation of Dilute Organic-Waters Mixtures—A Literature-Review on Modeling Studies and Applications to Aroma Compound Recovery. *J. Membr. Sci.* **1993**, *76*, 121−146.
(10) Williams, M. E.; Hestekin, J. A.; Smothers, C. N.; Bhattacharyya, D. Separation of Organic Pollutants by Reverse Osmosis and Nanofiltration Membranes: Mathematical Models and Experimental Verification. *Ind. Eng. Chem. Res.* **1999**, *38*, 3683−3695.
(11) Hartono, S. B.; Qiao, S. Z.; Jack, K.; Ladewig, B. P.; Hao, Z. P.; Lu, G. Q. Improving Adsorbent Properties of Cage-like Ordered Amine Functionalized Mesoporous Silica with Very Large Pores for Bioadsorption. *Langmuir* **2009**, *25*, 6413−6424.
(12) Sen, T.; Sebastianelli, A.; Bruce, I. J. Mesoporous Silica-Magnetite Nanocomposite: Fabrication and Applications in Magnetic Bioseparations. *J. Am. Chem. Soc.* **2006**, *128*, 7130−7131.
(13) Zhang, L.; Qiao, S. Z.; Jin, Y. G.; Yang, H. G.; Budihartono, S.; Stahr, F.; Yan, Z. F.; Wang, X. L.; Hao, Z. P.; Lu, G. Q. Fabrication and Size-Selective Bioseparation of Magnetic Silica Nanospheres with Highly Ordered Periodic Mesostructure. *Adv. Funct. Mater.* **2008**, *18*, 3203−3212.
(14) Kittur, A. A.; Kulkarni, S. S.; Aralaguppi, M. I.; Kariduraganavar, M. Y. Preparation and Characterization of Novel Pervaporation Membranes for the Separation Of Water−Isopropanol Mixtures using Chitosan and NaY Zeolite. *J. Membr. Sci.* **2005**, *247*, 75−86.
(15) Xu, Q.; Yang, Y.; Wang, X. Z.; Wang, Z. H.; Jin, W. Q.; Huang, J.; Wang, Y. Atomic Layer Deposition of Alumina on Porous Polytetrafluoroethylene Membranes for Enhanced Hydrophilicity and Separation Performances. *J. Membr. Sci.* **2012**, *415*, 435−443.
(16) Choi, J.; Jeong, H. K.; Snyder, M. A.; Stoeger, J. A.; Masel, R. I.; Tsapatsis, M. Grain Boundary Defect Elimination in a Zeolite Membrane by Rapid Thermal Processing. *Science* **2009**, *325*, 590−593.
(17) Ge, Q. Q.; Wang, Z. B.; Yan, Y. S. High-Performance Zeolite NaA Membranes on Polymer-Zeolite Composite Hollow Fiber Supports. *J. Am. Chem. Soc.* **2009**, *131*, 17056−17057.
(18) Kanezashi, M.; O'Brien-Abraham, J.; Lin, Y. S.; Suzuki, K. Gas Permeation through DDR-Type Zeolite Membranes at High Temperatures. *AIChE J.* **2008**, *54*, 1478−1486.
(19) Xu, L.; Lee, H. K. Zirconia Hollow Fiber: Preparation, Characterization, and Microextraction Application. *Anal. Chem.* **2007**, *79*, 5241−5248.
(20) Yoo, W. C.; Stoeger, J. A.; Lee, P. S.; Tsapatsis, M.; Stein, A. High-Performance Randomly Oriented Zeolite Membranes Using Brittle Seeds and Rapid Thermal Processing. *Angew. Chem., Int. Ed.* **2010**, *49*, 8699−8703.
(21) Huang, Y.; Baker, R. W.; Vane, L. M. Low-Energy Distillation-Membrane Separation Process. *Ind. Eng. Chem. Res.* **2010**, *49*, 3760−3768.
(22) Vane, L. M.; Alvarez, F. R.; Huang, Y.; Baker, R. W. Experimental Validation of Hybrid Distillation-Vapor Permeation Process for Energy Efficient Ethanol−Water Separation. *J. Chem. Technol. Biotechnol.* **2010**, *85*, 502−511.
(23) Vane, L. M.; Namboodiri, V. V.; Meier, R. G. Factors Affecting Alcohol−Water Pervaporation Performance of Hydrophobic Zeolite−Silicone Rubber Mixed Matrix Membranes. *J. Membr. Sci.* **2010**, *364*, 102−110.
(24) Dacosta, A. R.; Fane, A. G. Net-Type Spacers—Effect of Configuration on Fluid-Flow Path and Ultrafiltration Flux. *Ind. Eng. Chem. Res.* **1994**, *33*, 1845−1851.
(25) Jang, K. S.; Kim, H. J.; Johnson, J. R.; Kim, W. G.; Koros, W. J.; Jones, C. W.; Nair, S. Modified Mesoporous Silica Gas Separation Membranes on Polymeric Hollow Fibers. *Chem. Mater.* **2011**, *23*, 3025−3028.
(26) Hicks, J. C.; Jones, C. W. Controlling the Density of Amine Sites on Silica Surfaces Using Benzyl Spacers. *Langmuir* **2006**, *22*, 2676−2681.
(27) Hodgkins, R. P.; Ahniyaz, A.; Parekh, K.; Belova, L. M.; Bergstrom, L. Maghemite Nanocrystal Impregnation by Hydrophobic Surface Modification of Mesoporous Silica. *Langmuir* **2007**, *23*, 8838−8844.
(28) Melero, J. A.; van Grieken, R.; Morales, G. Advances in the Synthesis and Catalytic Applications of Organosulfonic-Functionalized Mesostructured Materials. *Chem. Rev.* **2006**, *106*, 3790−3812.
(29) Wight, A. P.; Davis, M. E. Design and Preparation of Organic−Inorganic Hybrid Catalysts. *Chem. Rev.* **2002**, *102*, 3589−3613.
(30) Chaikittisilp, W.; Kim, H. J.; Jones, C. W. Mesoporous Alumina-Supported Amines as Potential Steam-Stable Adsorbents for Capturing CO_2 from Simulated Flue Gas and Ambient Air. *Energy Fuels* **2011**, *25*, 5528−5537.
(31) Chaikittisilp, W.; Didas, S. A.; Kim, H. J.; Jones, C. W. Vapor-Phase Transport as a Novel Route to Hyperbranched Polyamine-Oxide Hybrid Materials. *Chem. Mater.* **2013**, *25*, 613−622.
(32) Chew, T. L.; Ahmad, A. L.; Bhatia, S. Ordered Mesoporous Silica (OMS) as an Adsorbent and Membrane for Separation of Carbon Dioxide (CO_2). *Adv. Colloid Interface Sci.* **2010**, *153*, 43−57.
(33) Kumar, P.; Ida, J. C.; Guliants, V. V. High Flux Mesoporous MCM-48 Membranes: Effects of Support and Synthesis Conditions on Membrane Permeance and Quality. *Microporous Mesoporous Mater.* **2008**, *110*, 595−599.
(34) Nishiyama, N.; Park, D. H.; Koide, A.; Egashira, Y.; Ueyama, K. A Mesoporous Silica (MCM-48) Membrane: Preparation and Characterization. *J. Membr. Sci.* **2001**, *182*, 235−244.
(35) Pedernera, M.; de la Iglesia, O.; Mallada, R.; Lin, Z.; Rocha, J.; Coronas, J.; Santamaria, J. Preparation of Stable MCM-48 Tubular Membranes. *J. Membr. Sci.* **2009**, *326*, 137−144.
(36) Sakamoto, Y.; Nagata, K.; Yogo, K.; Yamada, K. Preparation and CO_2 Separation Properties of Amine-Modified Mesoporous Silica Membranes. *Microporous Mesoporous Mater.* **2007**, *101*, 303−311.
(37) Lu, S. F.; Wang, D. L.; Jiang, S. P.; Xiang, Y.; Lu, J. L.; Zeng, J. HPW/MCM-41 Phosphotungstic Acid/Mesoporous Silica Composites as Novel Proton-Exchange Membranes for Elevated-Temperature Fuel Cells. *Adv. Mater.* **2010**, *22*, 971−976.
(38) McKeen, J. C.; Yan, Y. S.; Davis, M. E. Proton Conductivity of Acid-Functionalized Zeolite Beta, MCM-41, and MCM-48: Effect of Acid Strength. *Chem. Mater.* **2008**, *20*, 5122−5124.
(39) Park, S. J.; Lee, D. H.; Kang, Y. S. High Temperature Proton Exchange Membranes Based on Triazoles Attached onto SBA-15 Type Mesoporous Silica. *J. Membr. Sci.* **2010**, *357*, 1−5.
(40) Seshadri, S. K.; Alsyouri, H. M.; Lin, Y. S. Counter Diffusion Self Assembly Synthesis of Ordered Mesoporous Silica Membranes in Straight Pore Supports. *Microporous Mesoporous Mater.* **2010**, *129*, 228−237.
(41) Kumar, P.; Kim, S.; Ida, J.; Guliants, V. V. Polyethyleneimine-Modified MCM-48 Membranes: Effect of Water Vapor and Feed Concentration on N_2/CO_2 Selectivity. *Ind. Eng. Chem. Res.* **2008**, *47*, 201−208.

(42) Park, D. H.; Nishiyama, N.; Egashira, Y.; Ueyama, K. Separation of Organic/Water Mixtures with Silylated MCM-48 Silica Membranes. *Microporous Mesoporous Mater.* **2003**, *66*, 69−76.
(43) Kim, H. J.; Jang, K. S.; Galebach, P.; Gilbert, C.; Tompsett, G.; Conner, W. C.; Jones, C. W.; Nair, S. Seeded Growth, Silylation, and Organic/Water Separation Properties of MCM-48 Membranes. *J. Membr. Sci.* **2013**, *427*, 293−302.
(44) Brown, A. J.; Johnson, J. R.; Lydon, M. E.; Koros, W. J.; Jones, C. W.; Nair, S. Continuous Polycrystalline Zeolitic Imidazolate Framework-90 Membranes on Polymeric Hollow Fibers. *Angew. Chem., Int. Ed.* **2012**, *51*, 10615−10618.
(45) Belwalkar, A.; Grasing, E.; Van Geertruyden, W.; Huang, Z.; Misiolek, W. Z. Effect of Processing Parameters on Pore Structure and Thickness of Anodic Aluminum Oxide (AAO) Tubular Membranes. *J. Membr. Sci.* **2008**, *319*, 192−198.
(46) Collins, T. J. ImageJ for Microscopy. *Biotechniques* **2007**, *43*, 25−30.
(47) Al-Juaied, M.; Koros, W. J. Performance of Natural Gas Membranes in the Presence of Heavy Hydrocarbons. *J. Membr. Sci.* **2006**, *274*, 227−243.
(48) Vu, D. Q.; Koros, W. J.; Miller, S. J. High Pressure CO_2/CH_4 Separation Using Carbon Molecular Sieve Hollow Fiber Membranes. *Ind. Eng. Chem. Res.* **2002**, *41*, 367−380.
(49) Baker, R. W.; Wijmans, J. G.; Huang, Y. Permeability, Permeance and Selectivity: A Preferred Way of Reporting Pervaporation Performance Data. *J. Membr. Sci.* **2010**, *348*, 346−352.
(50) Beaurecard, G. P.; Hu, Y. H.; Grainger, D. W.; James, S. P. Silylation of Poly-L-Lysine Hydrobromide to Improve Dissolution in Apolar Organic Solvents. *J. Appl. Polym. Sci.* **2001**, *79*, 2264−2271.
(51) Bhatia, S. K. Modeling Pure Gas Permeation in Nanoporous Materials and Membranes. *Langmuir* **2010**, *26*, 8373−8385.
(52) Bhatia, S. K.; Nicholson, D. Some Pitfalls in the Use of the Knudsen Equation in Modelling Diffusion in Nanoporous Materials. *Chem. Eng. Sci.* **2011**, *66*, 284−293.
(53) Wu, S. F.; Wang, J. Q.; Liu, G. L.; Yang, Y.; Lu, J. M. Separation of Ethyl Acetate (EA)/Water by Tubular Silylated MCM-48 Membranes Grafted with Different Alkyl Chains. *J. Membr. Sci.* **2012**, *390*, 175−181.
(54) Baker, R. W.; Wijmans, J. G.; Huang, Y. Permeability, Permeance and Selectivity: A Preferred Way of Reporting Pervaporation Performance Data. *J. Membr. Sci.* **2010**, *348*, 346−352.
(55) Schoutens, G. H.; Groot, W. J. Economic-Feasibility of the Production of Iso-Propanol-Butanol-Ethanol Fuels from Whey Permeate. *Process Biochem.* **1985**, *20*, 117−121.
(56) Li, L.; Xiao, Z. Y.; Tan, S. J.; Liang, P.; Zhang, Z. B. Composite PDMS Membrane with High Flux for the Separation of Organics from Water by Pervaporation. *J. Membr. Sci.* **2004**, *243*, 177−187.
(57) Thiyagarajan, R.; Ravi, S.; Bhattacharya, P. K. Pervaporation of Methyl-Ethyl Ketone and Water Mixture: Determination of Concentration Profile. *Desalination* **2011**, *277*, 178−186.
(58) Zhan, X.; Li, J. D.; Huang, J. Q.; Chen, C. X. Enhanced Pervaporation Performance of Multi-layer PDMS/PVDF Composite Membrane for Ethanol Recovery from Aqueous Solution. *Appl. Biochem. Biotechnol.* **2010**, *160*, 632−642.
(59) Zhang, Q. G.; Hu, W. W.; Zhu, A. M.; Liu, Q. L. UV-Crosslinked Chitosan/Polyvinylpyrrolidone Blended Membranes for Pervaporation. *RSC Adv.* **2013**, *3*, 1855−1861.
(60) Tian, X. Z.; Jiang, X. Poly(vinylidene fluoride-*co*-hexafluoropropene) (PVDF-HFP) Membranes for Ethyl Acetate Removal from Water. *J. Hazard. Mater.* **2008**, *153*, 128−135.
(61) Shu, X. J.; Wang, X. R.; Kong, Q. Q.; Gu, X. H.; Xu, N. P. High-Flux MFI Zeolite Membrane Supported on YSZ Hollow Fiber for Separation of Ethanol/Water. *Ind. Eng. Chem. Res.* **2012**, *51*, 12073−12080.
(62) Tuan, V. A.; Li, S. G.; Noble, R. D.; Falconer, J. L. Preparation and Pervaporation Properties of a MEL-Type Zeolite Membrane. *Chem. Commun.* **2001**, *6*, 583−584.
(63) Sakaki, K.; Habe, H.; Negishi, H.; Ikegami, T. Pervaporation of Aqueous Dilute 1-Butanol, 2-Propanol, Ethanol and Acetone Using a Tubular Silicalite Membrane. *Desalin. Water Treat.* **2011**, *34*, 290−294.
(64) Negishi, H.; Sakaki, K.; Ikegami, T. Silicalite Pervaporation Membrane Exhibiting a Separation Factor of over 400 for Butanol. *Chem. Lett.* **2010**, *39*, 1312−1314.
(65) Chen, X. S.; Lin, X.; Chen, P.; Kita, H. Pervaporation of Ketone/Water Mixtures through Silicalite Membrane. *Desalination* **2008**, *234*, 286−292.
(66) Zhou, H. L.; Su, Y.; Chen, X. R.; Wan, Y. H. Separation of Acetone, Butanol and Ethanol (ABE) from Dilute Aqueous Solutions by Silicalite-1/PDMS Hybrid Pervaporation Membranes. *Sep. Purif. Technol.* **2011**, *79*, 375−384.
(67) Liu, X. L.; Li, Y. S.; Liu, Y.; Zhu, G. Q.; Liu, J.; Yang, W. S. Capillary Supported Ultrathin Homogeneous Silicalite-Poly-(Dimethylsiloxane) Nanocomposite Membrane for Bio-Butanol Recovery. *J. Membr. Sci.* **2011**, *369*, 228−232.